

High coercivity CoCrPt films achieved by post-deposition rapid thermal annealing

Jie Zou,^{a)} Bin Lu, Todd Leonhardt, David E. Laughlin, and David N. Lambeth
Data Storage System Center, Carnegie Mellon University, Pittsburgh, Pennsylvania 15213

Post-deposition rapid thermal annealing (RTA) was performed on multilayered films consisting of a Mn capping layer on top of CoCrPt/CrTi/NiAl. High coercivities were achieved even at low $M_r t$ values and coercivity values increased more than that would have been predicted by the decrease in magnetization values. This is most likely due to the significant decrease in intergranular exchange coupling, as shown by the δM measurement. Transmission electron microscopy characterization indicates no apparent grain growth and no visible improvement in CoCrPt crystallographic texture after RTA. It is believed that the preferential diffusion of Mn into CoCrPt grain boundaries promotes magnetic grain isolation. © 2000 American Institute of Physics.
 [S0021-8979(00)48208-3]

I. INTRODUCTION

Magnetic grain isolation is critical in obtaining low noise and high coercivity recording media. Cr segregation at the grain boundaries is a widely adopted approach to achieve magnetic isolation for a variety of CoCrX alloys. A relatively high Cr concentration is normally used to induce a significant Cr segregation, but the crystalline anisotropy energy is compromised,¹ which is unfavorable in achieving thermally stable high density media.

Since the grain boundary diffusion process is known to have a lower activation energy than bulk lattice diffusion, grain boundaries are fast channels for diffusion.^{2,3} Under certain processing conditions, it may be possible to diffuse sufficient underlayer materials to the magnetic grain boundaries while diffusing only a small amount into the bulk of the magnetic grains. Therefore, this may be a method of achieving grain isolation with only a moderate decrease in the anisotropy energy density.

A post-deposition RTA dramatically decreases the positive δM peak and increases the coercivity, while not significantly decreasing the anisotropy of the CrMn/CoCrPt/CrMn/NiAl and Cr/CoCrPt/Cr/NiAl films.^{4,5} Using CrMn had much larger effects on the improvement in magnetic properties than using Cr. This is consistent with Lee *et al.*'s original paper on CrMn underlayers⁶ and Peng *et al.*'s work on Mn or Cu overlayers.⁷

In this work, a sputtered film structure consisting of a NiAl underlayer, a CrTi intermediate layer, a CoCrPt magnetic layer, a capping Mn diffusion layer, and a final CrTi oxidation protection layer was investigated. CrTi was used to provide a better lattice match to the CoCrPt.⁸ The magnetic properties of the CoCrPt magnetic layer with various thicknesses after RTA treatment at different conditions were studied.

II. EXPERIMENT

All layers were deposited onto glass substrates by rf diode sputtering at 10 mTorr without substrate preheating. The

NiAl underlayer was 1000 Å thick. The thickness of the CoCrPt magnetic layer was varied from 50 to 300 Å. The CrTi intermediate layer, Mn capping layer, and CrTi oxidation protection layer were all 200 Å thick. Post-deposition annealing was performed at atmospheric pressure under Ar flow.

III. RESULTS AND DISCUSSION

Figure 1 shows typical magnetic data obtained for various annealing times. The annealing temperature was 350 °C and the magnetic layer thickness was 150 Å. The coercivity increased rapidly from 3200 to 5100 Oe after the 4 min annealing then slowly increased for longer annealing time. The $M_r t$ values decreased as the annealing time increased. The δM peak value initially decreased rapidly toward zero and then more slowly for longer annealing time, indicating the decrease in intergranular exchange coupling.⁹ The decrease in S^* with longer annealing time reflects the breakup of large magnetically coupled clusters of grains and reduced collective magnetic switching behavior, which is consistent with the reduction in intergranular exchange coupling. The same RTA treatment on the similar structured sample but without the Mn layer yielded no increase in H_c and no significant change in other magnetic properties. Thus the diffusion of Mn into the CoCrPt grain boundaries is most likely the main cause for the improvement in the magnetic properties.

Compared to the as-deposited values, the H_c increased 60%–73% and the $M_r t$ decreased only 22%–35%. The coercivity is normally viewed to be proportional to the anisotropy field H_k , as $H_c = CH_k$, where C is a constant depending on a variety of factors such as grain size, intergranular exchange coupling and magnetostatic coupling. A simple first-order uniaxial Stoner–Wohlfarth model yields $H_k = 2K_u/M_s$. Because the remanence squareness did not change much after the RTA, the M_s value should be approximately proportional to the $M_r t$ value, assuming that the thickness of the magnetic layer remained the same. Then K_u times the constant C is proportional to the product of H_c and $M_r t$. Hence, the product of the normalized H_c and $M_r t$ is

^{a)}Electronic mail: jzou@ece.cmu.edu

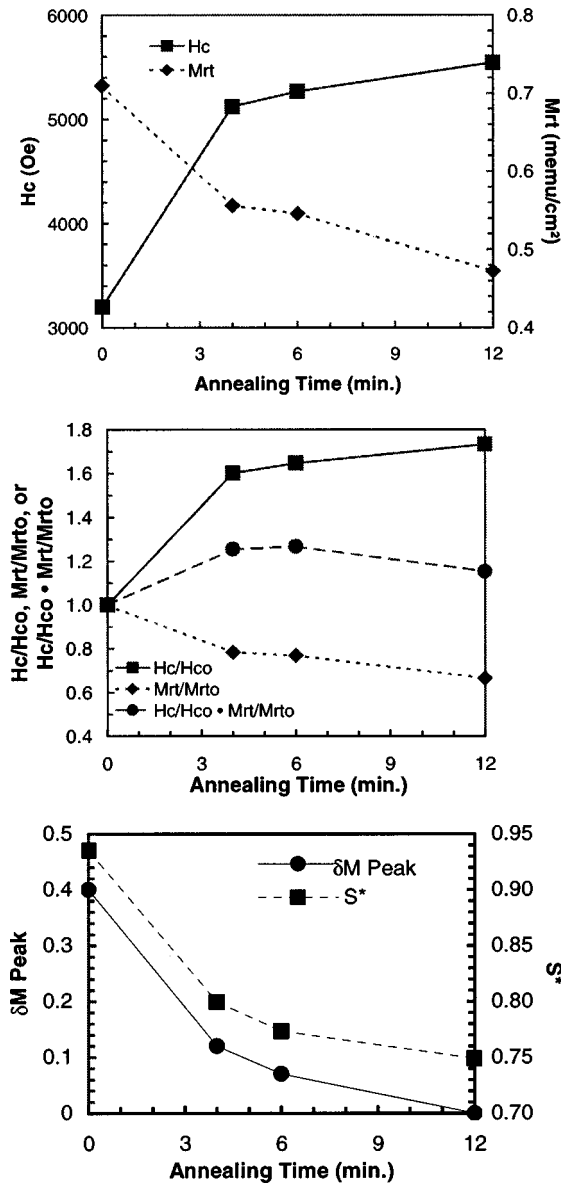


FIG. 1. H_c , $M_{r,t}$, normalized H_c , $M_{r,t}$, and their product, δM peak and S^* vs annealing time. H_{c0} and $M_{r,t0}$ are the as-deposited values.

plotted to show the contributions to the increase of the coercivity other than that due to the decrease in the magnetization. This product had a maximum at the annealing time of 6 min; which is consistent with the diffusion kinetics. The diffusion process in a polycrystal can be characterized as rapid diffusion down the grain boundaries with simultaneous lateral leakage diffusion into the adjoining grains.² The diffusion of the nonmagnetic materials into the CoCrPt grain boundaries promotes the Co-alloy grain isolation and thus increases the constant C . However, it is anticipated that K_u may start to decrease as a significant amount of the nonmagnetic materials leak into the bulk of the CoCrPt grains.

Figure 2 shows the magnetic properties vs the CoCrPt thickness. The annealing conditions, at which the δM peak dropped below 0.1, are shown in Table I. As expected, the annealing time strongly depended on the magnetic layer thickness. For the 300-Å-thick CoCrPt sample, it was found that more than 3 min. was required at the temperature of

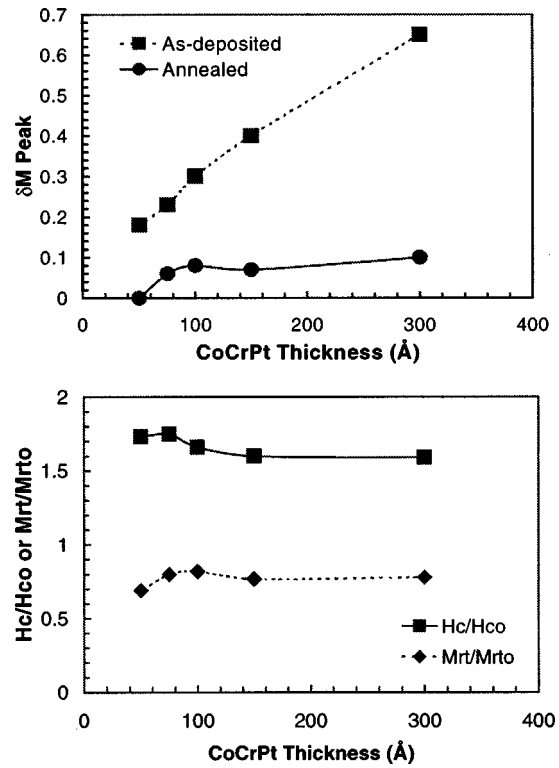


FIG. 2. The δM peak and normalized H_c and $M_{r,t}$ vs CoCrPt thickness. H_{c0} and $M_{r,t0}$ are the as-deposited values.

350 °C. Thus, the annealing temperature was increased to 400 °C to shorten the annealing time.

The coercivity increased 60%–75% and the $M_{r,t}$ decreased only 18%–30% after RTA. Post-deposition annealing decreased the δM peak for all the samples with different thicknesses. However, the δM peak values for the as-deposited films also decreased with thinner CoCrPt thickness. This may be due to the preferential diffusion of Mn from the capping layer into the CoCrPt magnetic grain boundaries caused by the heating from the rf-sputtering process. The penetration depth of Mn into the Co-alloy grain boundaries is expected to be about the same for all samples, but would be a larger fraction of the total magnetic layer thickness for the thinner CoCrPt samples. Therefore, the resulted grain isolation for thinner Co-alloy layers would be more effective.

Figure 3 shows the H_c vs $M_{r,t}$ curves for as-deposited and annealed samples. The coercivity decreased with decreasing $M_{r,t}$ value, for both curves. However, for the annealed samples, the coercivity was still as high as 4400 Oe for an $M_{r,t}$ value as low as 0.27 memu/cm².

TABLE I. The annealing conditions for the samples shown in Fig. 2.

CoCrPt thickness (Å)	Annealing temperature (°C)	Annealing time (min.)
50	350	0.5
75	350	1
100	350	2
150	350	6
300	400	3

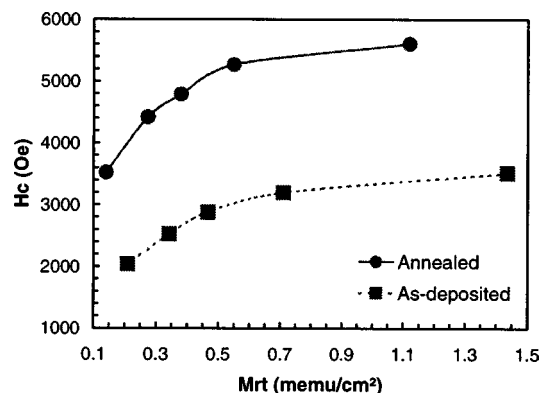


FIG. 3. H_c vs $M_{r,t}$ for as-deposited and annealed samples.

Figure 4 shows the plane-view TEM bright-field images of the 150-Å-thick CoCrPt magnetic layer, for both the as-deposited and the annealed at 350 °C for 6 min samples. Comparing these two images, no apparent grain growth is visible. The visual estimate of the average CoCrPt grain size for both is about 20 nm. The dark area in the TEM image of

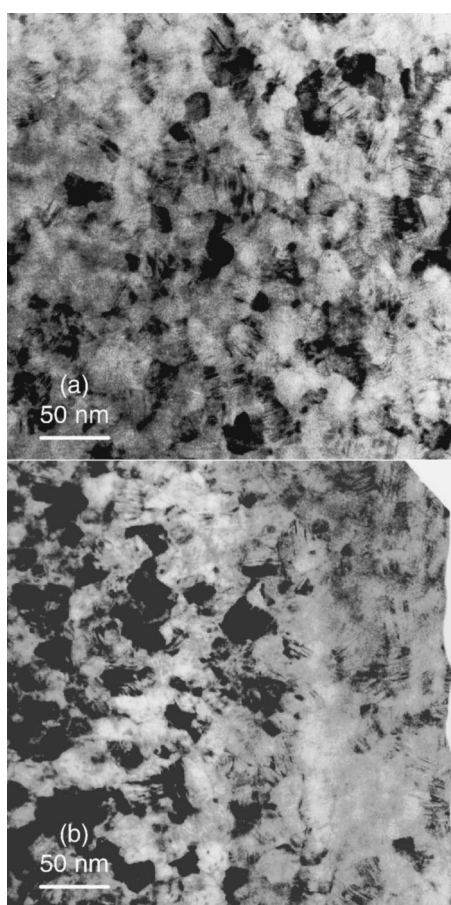


FIG. 4. Plane-view bright-field TEM image of (a) as-deposited and (b) annealed samples.

TABLE II. The CoCrPt (10 $\bar{1}$ 0) texture axis distribution angles for as-deposited and annealed samples. The CoCrPt thickness was 150 Å.

Sample	Co (10 $\bar{1}$ 0) texture axis distribution angle
As-deposited	12° ± 1°
Annealed at 350° C for 6 min.	12° ± 1°

the annealed sample was thicker where a portion of the CrTi intermediate layer remained, while the lighter area was only of the CoCrPt layer. In the as-deposited sample image, there was only the Co-alloy layer.

The effect of RTA on crystallographic texture of CoCrPt was also studied. The tilting electron diffraction technique was used to measure the CoCrPt (10 $\bar{1}$ 0) texture axis distribution angle.^{10,11} The results were shown in Table II. The Co-alloy (10 $\bar{1}$ 0) texture distribution angles were the same for the as-deposited and annealed samples, indicating that no significant change in Co-alloy growth texture was induced by the RTA treatment.

IV. CONCLUSION

High coercivities were achieved by post-deposition annealing of CoCrPt/CrTi/NiAl films with Mn capping layers. The coercivity was 4400 Oe for an $M_{r,t}$ value as low as 0.27 memu/cm² and was higher than 5000 Oe for $M_{r,t}$ larger than 0.5 memu/cm². The intergranular exchange coupling was effectively decreased by the RTA process. No apparent grain growth and texture change in the CoCrPt magnetic layers was found after annealing. The diffusion of Mn into CoCrPt magnetic grain boundaries probably plays the key role in the improvement of the grain isolation.

¹N. Inaba, M. Futamoto, and A. Nakamura, *IEEE Trans. Magn.* **34**, 1558 (1998).

²I. Kaur and W. Gust, *Fundamentals of Grain and Interphase Boundary Diffusion*, 2nd ed. (Ziegler, Stuttgart, 1989), Chaps. 1 and 2.

³D. Gupta, in *Diffusion Phenomena in Thin Films and Microelectronic Materials*, edited by D. Gupta and P. S. Ho (Noyes, Park Ridge, NJ, 1988), pp. 33–51.

⁴J. Zou, D. E. Laughlin, and D. N. Lambeth, *Mater. Res. Soc. Symp. Proc.* **517**, 217 (1998).

⁵J. Zou, B. Lu, D. E. Laughlin, and D. N. Lambeth, *IEEE Trans. Magn.* **35**, 2661 (1999).

⁶L.-L. Lee, D. E. Laughlin, and D. N. Lambeth, *IEEE Trans. Magn.* **34**, 1561 (1998).

⁷W. Peng, Z. Qian, C. Yang, J. Sivertson, and J. H. Judy, *J. Appl. Phys.* **85**, 4702 (1999).

⁸Y. Shiroishi, Y. Hosoe, A. Ishikawa, Y. Yahisa, Y. Sugita, H. Suzuki, T. Ohno, and M. Ohura, *J. Appl. Phys.* **73**, 5569 (1993).

⁹P. I. Mayo, K. O. Grady, P. E. Kelly, J. A. Cambridge, I. L. Sanders, T. Yogi, and R. W. Chantrell, *J. Appl. Phys.* **69**, 4733 (1991).

¹⁰L. Tang, Y. C. Feng, L.-L. Lee, and D. E. Laughlin, *J. Appl. Crystallogr.* **29**, 419 (1996).

¹¹B. Lu, D. E. Laughlin, D. N. Lambeth, S. Z. Wu, R. Ranjan, and G. C. Rauch, *J. Appl. Phys.* **85**, 4295 (1999).